Application of the FSA scaling method to the LSTF ROSA 1.2 test and comparison to an application of the H2TS method

Antoine Ciechocki, Sofia Carnevali, Dominique Bestion, Lionel Rossi

APPLICATION OF THE FSA SCALING METHOD TO THE LSTF ROSA 1.2 TEST AND COMPARISON TO AN APPLICATION OF THE H2TS METHOD

A. Ciechocki*, S. Carnevali
Commissariat à l'énergie atomique et aux énergies alternatives
Centre CEA Paris-Saclay - 91191 Gif-sur-Yvette Cedex, France
antoine.ciechocki@cea.fr; sofia.carnevali@cea.fr

D. Bestion
Consultant
22 Avenue de l'Europe, 38120, Saint Egrève, France
dominique.bestion@wanadoo.fr

L. Rossi
Commissariat à l'énergie atomique et aux énergies alternatives
Centre CEA Cadarache - 13115 Saint-Paul-lez-Durance, France
lionel.rossi@cea.fr

ABSTRACT

The general objective of this work is to compare scaling methods and some different ways to apply them. In the present work, an application of the Fractional Scaling Analysis (FSA) method is compared to an application of the Hierarchical Two-Tiered Scaling (H2TS) method done by the Polytechnic University of Valence (UPV). The ROSA 1.2 test performed on the Japanese LSTF-ROSA-IV facility is analyzed. It is a 1% Hot Leg break LOCA. This transient is divided into five phases. Important bifurcating events are identified. A scaling analysis is applied to the first and the fourth phases called respectively the blowdown and the high-quality mixture discharge. The blowdown starts at the break opening while high-quality mixture discharge starts when primary and secondary pressures cross. The FSA methodology is applied at system and component scale by writing mass and pressure equations for two different control volumes, the primary system and the pressurizer. The CATHARE system thermal hydraulic code is used to calculate the effect metrics, scaling criteria specific to this method, which are analyzed and compared with the π-groups of the H2TS, obtained by the application of the UPV with the TRACE code. Differences between the results of the two methods are discussed. Moreover, the relative weight of the processes that control the pressure are evaluated. Some conclusions are drawn on the scaling and possible distortions of the test facility.

KEYWORDS
SB-LOCA, Scaling, LSTF, FSA, H2TS

* PhD student at Université Paris-Saclay, SMEMaG (ED579)

1. INTRODUCTION

The “scaling’’ activity is involved in several steps of a thermal hydraulic analysis of a nuclear reactor accidental transient [1]. Experimental test facilities are necessary to simulate reactor transients. Experiments are performed to identify and understand the transient phenomena, and to support the validation of the numerical simulation tools. Since no full-size experimental test reactor is affordable, scaling methods are used to design reduced scale facilities and to define test conditions able to represent the behavior in the full-size reference reactor with minimal distortions. The scaling method uses a ranking of processes with respect to their impact on the Figures of Merit (FoM) of the transient in order to respect the similarity of the dominant (highly ranked) processes in the test design, and to estimate the distortions of the other processes. Scaling is also used to give requirements to code models, which should well describe dominant processes, and to define the validation matrix of the code. The code validation is done by comparing the results of the code predictions with experimental data. Codes should predict correctly dominant processes, and the scale effect of all influent processes to be able to do the transposition to the reactor transient. This is called the code scalability or code capability to do the “scaling-up’’.

The majority of Integral Test Facilities (ITF) are scaled based on respecting power-to-volume ratio and respecting the full-height of the reactor (e.g. BETHSY, LSTF, LOBI, SPES). Then came the three-level scaling [2] with reduced height and a reduction of the time scale. With the need to design facilities with reduced height and pressure, the power-to-mass scaling method was developed [3]. Later, other types of methods intended for scale transposition and to support system codes were developed. The Hierarchical Two-Tiered Scaling methodology (H2TS) introduced the first concepts of hierarchy and scaling groups [4]. Thereafter, the Fractional Scaling Analysis (FSA) was developed as an improvement of the H2TS [5]. Finally, the recent Dynamical System Scaling method (DSS), similar to the H2TS and FSA was developed [6].

The H2TS method introduces the concept of top-down approach followed by the bottom-up approach [4]. The top-down step (also called stepwise design) starts the scaling analysis for an Integral Effect Test (IET) at the global system scale, in view of defining the scaling ratios for the core power, the total system volume, and the nominal flow rate. The analysis divides the whole system into individual parts and considering progressively smaller scales, i.e. the component scale, the sub-component scale, to the local process scale. Then, the bottom-up step is the reverse process, which brings together individual information about the IET design, from basic building blocks to the complex system. In the field of the study of nuclear transients, these two steps allow a comprehensive method for the scaling analysis. It was also claimed that this approach provides efficiency through cost-effective and timely resolution [7]. However, advanced methods such as H2TS and FSA require a high level of expertise in transient analysis and a deep understanding of two-phase thermal hydraulics. No handbook for scaling method exists and guidance on how to apply them is required. This work intends to clarify how they can be applied, to compare their merits, to identify the difficulties, and to see how system codes can support the scaling analysis.

The Small-Break Loss Of Coolant Accidents (SB-LOCAs) became important in reactor safety analysis after the Three Miles Island (TMI) accident. It is chosen to revisit a posteriori the scaling of an already existing SB-LOCA integral test using all the available knowledge and tools including the results of the test and the results of a system code simulation. A scaling analysis is performed using the FSA method and it is compared to an application of the H2TS method done by the Polytechnic University of Valence (UPV) [8]. Some differences and similarities of these two methods will be identified to highlight the cause and importance of the choices that can be made during a scaling analysis.

The scaling analysis is carried out on the ROSA 1.2 test performed on the Japanese LSTF-ROSA-IV facility. In this study, the thermal hydraulic system code used is the CATHARE code [9][10][11]. The UPV uses the TRACE code.

2. BRIEF DESCRIPTION OF THE ROSA 1.2 TEST

2.1. The LSTF Facility

The ROSA 1.2 test was performed on the Large Scale Test Facility (LSTF) of the Japan Atomic Energy Research Institute (JAERI) [12][13]. LSTF is designed to simulate a Westinghouse four loops PWR with a full power of 3423 MWt – 1100 MWe. As shown in Figure 1, LSTF has two loops, two steam generators and one pressurizer. The facility was designed using the same scaling factor for power and volume, a full-height scaling, and a 1/48 scaled volume at full-pressure reference condition. The maximum core power is equal to 14% of the 1/48 nominal power of the reference reactor i.e. 10 MWt. This scaling respects the timing of events. The flow area is 1/48 scaled in the pressure vessel and 1/24 scaled in the cold and hot legs (HL & CL) and in the steam generators (SG) since each loop represents two reactor loops.

This work will use the simulation of the ROSA 1.2 test using the CATHARE system code [9]. The model contains the primary and the secondary systems. The primary side contains the Reactor Pressure Vessel (RPV), two hot and cold legs with main coolant pumps, the pressurizer and the U-tubes of the two steam generators. The system also includes High Pressure Injection System (HPIS) and Accumulator Injection Systems (AIS). The nodalization of the LSTF primary system with CATHARE is shown in Figure 1.

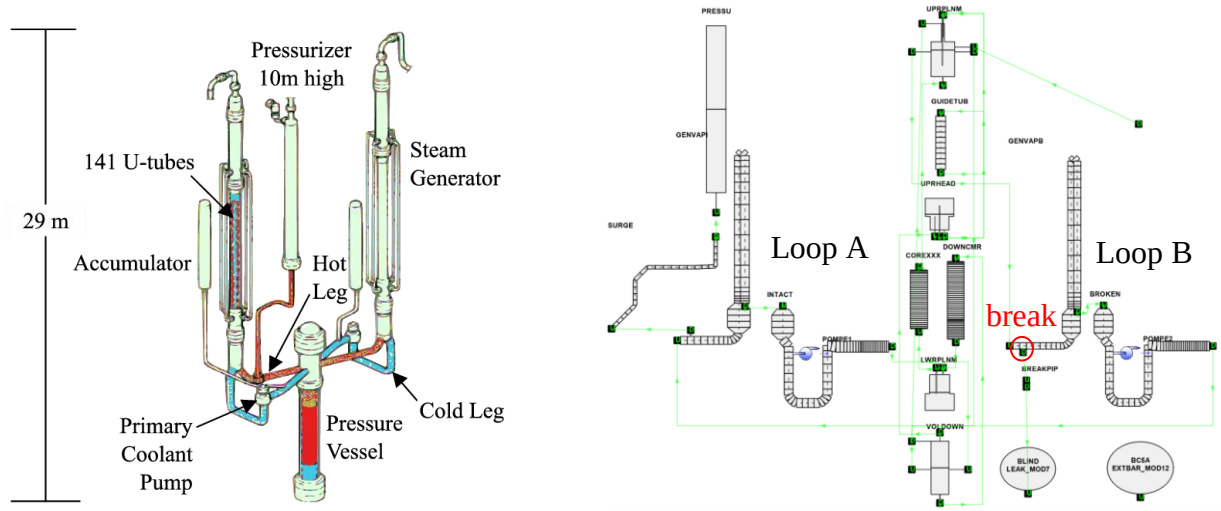

Figure 1. Large Scale Test Facility (LSTF) used for the ROSA 1.2 test and the CATHARE nodalization of the primary system

2.2. The SB-LOCA Transient

The ROSA 1.2 test scenario consists of a SB-LOCA experiment. The break corresponds to 1% of the volumetrically scaled cross-sectional area of the reference reactor cold leg. The break is located on the hot leg of the loop without pressurizer.

The test starts at operating full-pressure of 15.5 MPa and at a nominal power of 10 MWt. The reactor SCRAM signal occurs at 12.97 MPa resulting in the core power decay. The main coolant pumps gradually stop as well as the pressurizer heaters and the secondary feed water. At a pressure of 12.27 MPa, the safety injection signal triggers the HPIS pumps with a 12 seconds delay. The accumulator injection system (AIS) is activated at 4.51 MPa.

At the break opening, the primary fluid is discharged first in liquid state. With decreasing pressure and decreasing mass inventory, the steam quality of discharged fluid at the break gradually increases. Throughout the transient, the main concern is the core cooling which may be challenged when a partially uncovered core induces a clad temperature excursion. This event mainly depends on the primary mass inventory, which itself depends a lot on the primary pressure evolution that influences the break flow rate and the safety injections. These two parameters are thus essential to describe the SB-LOCA transient.

The transient is divided into five chronological phases. These phases, also called "phenomenological windows", depend on the phenomena and on system parameters evolution. Bifurcating events that correspond to abrupt changes of phenomena, delimit the phases. In the literature, usually 3, 4 or 5 phase splits, characterized by physical processes and phenomena, are defined for SB-LOCA transients. In the current study, the SB-LOCA is divided into 5 phases following the UPV analysis [8]. This choice allows separation of the dominant processes throughout the transient. They are presented in Figure 2 describing the evolution of the primary and secondary pressure as well as the primary mass inventory. The bifurcating events are summarized in Table I.

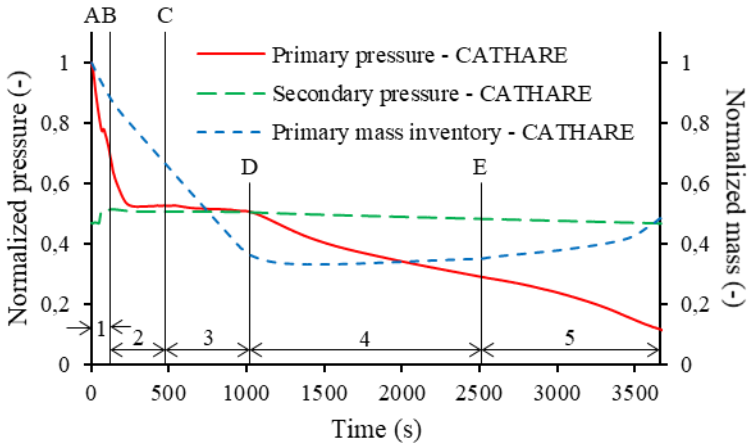

Figure 2. Primary and secondary evolutions during the phases of a SB-LOCA

Table I. SB-LOCA phases and bifurcating events

Phases	Bifurcating events
1. Blowdown Discharge (BD)	A. Break opening
2. Natural Circulation (NC)	B. Pressurizer emptied, pump stop
3. Two-Phase Discharge (TPD)	C. Top of SG tubes emptied (no liquid flow)
4. High-Quality Mixture Discharge (HQMD)	D. Primary-secondary pressure reversal
5. Reactor Refilling (RR)	E. Accumulator discharge

1. The Blowdown Discharge phase:

After the opening of the break, the primary system depressurizes quickly from 15.5 MPa to 10.7 MPa in 119 seconds. The primary system remains liquid in the loops and in the pressure vessel up to 60 seconds. Flashing occurs first in the pressurizer due to its higher temperature. The SCRAM signal triggers at around 50 seconds and the core power will join a decay power curve, which is truncated at 14%. The primary pumps are stopped and the rotation speed gradually decreases depending on the flywheel, initiating the transition to the natural circulation. The end of the blowdown discharge is defined as the emptying of the pressurizer (less than 1% of the initial liquid mass).

2. The Natural Circulation phase:
The pumps being stopped, the fluid circulation is due to the differences in density between the ascending and descending parts of the system. The ascending part is the core, the upper plenum, the hot legs and the ascending part of the steam generators U-tubes. The descending part is the descending part of the steam generators U-tubes, the cold legs, and the vessel downcomer. The difference of gravity in the ascending and descending parts of the circuit are compensated by friction and singular pressure losses along the loop. During this phase, the primary pressure decreases slowly (from 10.7 MPa to 8.2 MPa) and stays above the secondary pressure to be able to transfer energy to the steam generator (SG). During this phase, the core provides more energy to the fluid than is lost at the break and the primary fluid needs to give the rest of power to the SG. This requires a higher temperature and higher pressure than inside the SG.

3. The Two-Phase Discharge phase:
The vapour created in the core condenses in the steam generators U-tubes and the condensate water is first entrained in co-current flow to the intermediate leg (IL) and the cold leg. Then the mass of water decreasing, the void fraction increases in SG tubes and the vapour is no more capable to entrain the condensate water to the top of the SG tubes. This is the end of the natural circulation (NC) and the beginning of the Reflux Condenser Mode (RCM). Some decay power is still removed by condensation in the SG, with the condensate water flowing back to the hot legs in the ascending part of SG tubes whereas the condensate in the descending part of SG tubes fills the intermediate legs. With the stop of NC, water tends to settle in the lower part of the circuit, the steam quality at the break increases and more power is evacuated at the break. Note that the Loop Seal Plugging (LSP) occurs without Loop Seal Clearing (LSC) during the 5 phases considered. During this Two-Phase Discharge, the primary pressure drops from 8.2 MPa to 7.7 MPa in 581 seconds.

4. The High-Quality Mixture Discharge phase:
The beginning of this phase is marked by the passage of the primary pressure below the secondary pressure. From this moment, the heat flux at the steam generators U-tubes is reversed. The gradual decrease of primary pressure increases the HPIS flow rate. The vapour condensation on the cold injected water increases the depressurization rate. During this phase, the pressure decreases significantly, from 7.7 MPa to 4.5 MPa in 1484 seconds. The liquid level in hot legs goes down until it reaches the height of the break. The discharge at the break is then almost vapour.

5. The Reactor Refilling phase:
This phase starts when the accumulator injection is triggered. A large flow rate of sub-cooled liquid is discharged into the primary system thanks to AIS and HPIS. From the beginning to the end of the accumulator discharge, the pressure decreases from 4.5 MPa to 1.8 MPa in 1148 seconds and the mass inventory starts increasing.

3. TOP-DOWN SCALING WITH FSA METHOD

The FSA methodology [5] is first applied to the blowdown and high-quality mixture discharge phases. For the SB-LOCA transient, the Figure of Merit (FoM) is defined as the Peak Clad Temperature (PCT) [1][5]. The most important Parameters of Interest (PoI) that influence the FoM are the mass inventory M and the primary pressure P_1. Equations will then be written for the primary mass evolution and for the primary pressure evolution. The primary pressure is first controlled by the pressurizer until it is empty, and then it is controlled by the mass and energy exchanges in the whole primary circuit.

3.1. Mass Balance Equations in a Volume V

The mass balance equation in a constant volume V is given by:

$$\frac{dM}{dt} \triangleq \dot{M} = \dot{M}_{in} - \dot{M}_{out} \tag{1}$$

$\dot{M}$ is the time rate change of fluid mass in V. $\dot{M}_{in}$ and $\dot{M}_{out}$ are respectively the mass flow rates entering and leaving V through fluid boundaries A_f. For a two-phase case, this equation can be split into liquid and vapour contributions. Mass balance equation becomes:

$$\dot{M} = \dot{M}_l + \dot{M}_v = \dot{M}_{l,in} - \dot{M}_{l,out} + \dot{M}_{v,in} - \dot{M}_{v,out} \tag{2}$$

The Eq. (2) applied to the pressurizer and the primary system gives respectively Eq. (3) and (4):

$$\dot{M}_{prz} = - \dot{M}_{l,prz,out} - \dot{M}_{v,prz,out} \tag{3}$$

$$\dot{M}_1 = \dot{M}_{l,HPIS} - \dot{M}_{l,break} - \dot{M}_{v,break} \tag{4}$$

Each contributor to the mass rate of change $\dot{M}$ is normalized with time-averaged of variables $\bar{Y}$ during the phases. Although the FSA method recommends normalization with an initial value Y_0 [5], it is chosen here to use this average calculated values by a code.

$$Y^+(t) = \frac{Y(t)}{\bar{Y}} \tag{5}$$

The Eq. (3) and (4) then writes respectively, introducing the Fractional Rate of Change (FRC) $\omega_{\dot{M},j}$:

$$\left.\frac{dM^+}{dt}\right|_{prz} = - \omega_{\dot{M}_{l,prz,out}} \cdot \dot{M}^+_{l,prz,out} - \omega_{\dot{M}_{v,prz,out}} \cdot \dot{M}^+_{v,prz,out} \tag{6}$$

$$\left.\frac{dM^+}{dt}\right|_{1} = \omega_{\dot{M}_{l,HPIS}} \cdot \dot{M}^+_{l,HPIS} - \omega_{\dot{M}_{l,break}} \cdot \dot{M}^+_{l,break} - \omega_{\dot{M}_{v,break}} \cdot \dot{M}^+_{v,break} \tag{7}$$

The normalized mass balance equation is obtained, function of the j Agents of Change $\phi^+_{\dot{M},j}$ which define the processes acting on $\dot{M}$:

$$\left.\frac{dM^+}{dt}\right|_{prz} = - \omega_{\dot{M}_{l,prz,out}} \cdot \phi^+_{\dot{M}_{l,prz,out}} - \omega_{\dot{M}_{v,prz,out}} \cdot \phi^+_{\dot{M}_{v,prz,out}} \tag{8}$$

$$\left.\frac{dM^+}{dt}\right|_{1} = \omega_{\dot{M}_{l,HPIS}} \cdot \phi^+_{\dot{M}_{l,HPIS}} - \omega_{\dot{M}_{l,break}} \cdot \phi^+_{\dot{M}_{l,break}} - \omega_{\dot{M}_{v,break}} \cdot \phi^+_{\dot{M}_{v,break}} \tag{9}$$

3.2. Pressure Equations in a Volume V

Let's now write the first principle of thermodynamics in a constant volume V with constant boundaries A to derive a total energy equation:

$$\frac{d}{dt}\int_V \rho\left(e+\frac{u^2}{2}\right)dV = \int_V \rho\left(\vec{F}\cdot\vec{u}+q_{ext}\right)dV - \int_{A_f} \rho\left(e+\frac{u^2}{2}\right)\vec{u}\cdot\vec{n}\,dA - \int_A \vec{q}\cdot\vec{n}\,dA - \int_{A_f}\left(\bar{\bar{T}}\cdot\vec{u}\right)\cdot\vec{n}\,dA \qquad (10)$$

Some simplifications are considered by neglecting the kinetic energy, the heat flux along fluid boundaries, the work of the gravity forces ($\vec{F}\cdot\vec{u}$) and radiative sources q_{ext}. Finally, the energy balance is expressed using enthalpy h instead of internal energy ($h=e+\frac{p}{\rho}$). The two-phase energy balance equation for a volume V writes:

$$\frac{dM_l\cdot H_l}{dt} + \frac{dM_v\cdot H_v}{dt} - V\frac{dP}{dt} = W_w + \dot{M}_{l,in}\cdot h_{l,in} - \dot{M}_{l,out}\cdot H_l + \dot{M}_{v,in}\cdot h_{v,in} - \dot{M}_{v,out}\cdot H_v \qquad (11)$$

With P the volume averaged pressure, $h_{l,in}$ and $h_{v,in}$ the liquid and vapour entering enthalpies and W_w the thermal power received from the walls. It is considered that the phases leaves the volume with the mass weighted averaged enthalpy H_k of the volume.

Taking into account the energy balance at the interfaces, the mass balance equation and a constant volume equation, is obtained [14] a pressure equation expressed in terms of fluid volume rate of change:

$$\begin{aligned}\left(\mu_l\cdot M_l + \mu_v\cdot M_v\right)\cdot\dot{P} &= \dot{M}_{l,in}\cdot\left[v_l + v'_{l,h}\cdot\left(h_{l,in} - H_l\right)\right] + \dot{M}_{v,in}\cdot\left[v_v + v'_{v,h}\cdot\left(h_{v,in} - H_v\right)\right] \\ - \dot{M}_{l,out}\cdot v_l - \dot{M}_{v,out}\cdot v_v &+ v'_{l,h}\cdot W_{w,l} + v'_{v,h}\cdot W_{w,v} + v'_{l,h}\cdot W_{i,l} + v'_{v,h}\cdot W_{i,v} - \frac{W_{i,v}+W_{i,l}}{\varpi} + \frac{W_{w,i}}{\varpi}\end{aligned} \qquad (12)$$

With:

$$v'_{k,p} \triangleq \left.\frac{\partial v_k}{\partial p}\right|_{h_k} \;;\; v'_{k,h} \triangleq \left.\frac{\partial v_k}{\partial h_k}\right|_{p} \;;\quad \mu_k = - v'_{k,p} - v_k\cdot v'_{k,h} \;;\; \varpi \triangleq \frac{h_v - h_l}{v_v - v_l}$$

Each term of the equation is a volume rate of change (VRC, in m^3/s). The term on the l.h.s is the fluid expansion in depressurization. The terms on r.h.s are the entering liquid and vapour volume flow rates and the associated thermal expansion when mixing with internal fluid, the VRC by exiting liquid and vapour flow rates, the VRC by liquid and vapour thermal expansion by wall heating and by interfacial exchanges, the VRC by vaporization or condensation, and the VRC by wall boiling or condensation. This formulation provides an easy interpretation of the impact of fluid volume changes on pressure. Fluid volume may change by source or sink of fluid at boundaries, by expansion/contraction by heat exchanges and by isentropic expansion/contraction.

In situations where both phases are close to the saturation, a simpler pressure equation assuming thermal equilibrium is written:

$$\begin{aligned}\left(\lambda_l\cdot M_l + \lambda_v\cdot M_v\right)\cdot\dot{P} = \dot{M}_{l,in}\cdot\left(v_{ls}+\frac{h_{l,in} - h_{ls}}{\varpi_s}\right) + \dot{M}_{v,in}\cdot\left(v_{vs}+\frac{h_{v,in} - h_{vs}}{\varpi_s}\right) \\ - \dot{M}_{l,out}\cdot v_{ls} - \dot{M}_{v,out}\cdot v_{vs} + \frac{W_w}{\varpi_s}\end{aligned} \qquad (13)$$

With:

$$\lambda_k = \frac{h'_{ks,p}}{\varpi_s} - \frac{v_{ks}}{\varpi_s} - v'_{ks,p} \;;\; \varpi_s \triangleq \frac{h_{vs} - h_{ls}}{v_{vs} - v_{ls}} \;;\; h'_{ks,p} \triangleq \frac{dh_{ks}}{dp} \;;\; v'_{ks,p} \triangleq \frac{dv_{ks}}{dp}$$

In this case, the l.h.s term represents all VRC due to expansion (or contraction) by pressure change; it includes isentropic expansion plus vaporization by flashing and thermal expansion following saturation curve.

The Eq. (13) applied to the pressurizer and the primary system gives respectively Eq. (14) and (15):

$$(\lambda_l \cdot M_l + \lambda_v \cdot M_v) \cdot \dot{P}_{prz} = - \dot{M}_{l,prz,out} \cdot v_{ls} - \dot{M}_{v,prz,out} \cdot v_{vs} + \frac{W_{prz,heaters}}{\varpi_s} + \frac{W_{prz,ow}}{\varpi_s} \tag{14}$$

$$\begin{aligned}(\lambda_l \cdot M_l + \lambda_v \cdot M_v) \cdot \dot{P}_1 = {} & \dot{M}_{l,HPIS} \cdot v_{ls} + \dot{M}_{l,HPIS} \cdot \frac{(h_{l,HPIS} - h_{ls})}{\varpi_s} \\ & - \dot{M}_{l,break} \cdot v_{ls} - \dot{M}_{v,break} \cdot v_{vs} + \frac{W_{core}}{\varpi_s} + \frac{W_{1,ow}}{\varpi_s} - \frac{W_{SG}}{\varpi_s}\end{aligned} \tag{15}$$

To simplify the VRC due to the pressure change, the global expansion coefficient K_s is defined:

$$K_s = (\lambda_l \cdot M_l + \lambda_v \cdot M_v) \tag{16}$$

Each contributor to the pressure rate of change $\dot{P}$ is normalized in the same way as above (5). The Eq. (14) and (15) then writes respectively, introducing the Fractional Rate of Change (FRC) $\omega_{\dot{P},j}$:

$$\begin{aligned}\left.\frac{dP^+}{dt}\right|_{prz} = {} & - \omega_{\dot{P},Q_{l,prz,out}} \cdot \frac{\dot{M}^+_{l,prz,out} \cdot v^+_{ls}}{K^+_s} - \omega_{\dot{P},Q_{v,prz,out}} \cdot \frac{\dot{M}^+_{v,prz,out} \cdot v^+_{vs}}{K^+_s} \\ & + \omega_{\dot{P},Q_{prz,heaters}} \cdot \frac{W^+_{prz,heaters}}{K^+_s \cdot \varpi^+_s} + \omega_{\dot{P},Q_{prz,ow}} \cdot \frac{W^+_{prz,ow}}{K^+_s \cdot \varpi^+_s}\end{aligned} \tag{17}$$

$$\begin{aligned}\left.\frac{dP^+}{dt}\right|_1 = {} & \omega_{\dot{P},Q_{l,HPIS}} \cdot \frac{\dot{M}^+_{l,HPIS} \cdot v^+_{ls}}{K^+_s} + \omega_{\dot{P},Q_{cond,HPIS}} \cdot \frac{\dot{M}^+_{l,HPIS} \cdot (h^+_{l,HPIS} - h^+_{ls})}{K^+_s \cdot \varpi^+_s} - \omega_{\dot{P},Q_{l,break}} \cdot \frac{\dot{M}^+_{l,break} \cdot v^+_{ls}}{K^+_s} - \\ & \omega_{\dot{P},Q_{v,break}} \cdot \frac{\dot{M}^+_{v,break} \cdot v^+_{vs}}{K^+_s} + \omega_{\dot{P},Q_{core}} \cdot \frac{W^+_{core}}{K^+_s \cdot \varpi^+_s} + \omega_{\dot{P},Q_{1,ow}} \cdot \frac{W^+_{1,ow}}{K^+_s \cdot \varpi^+_s} - \omega_{\dot{P},Q_{SG}} \cdot \frac{W^+_{SG}}{K^+_s \cdot \varpi^+_s}\end{aligned} \tag{18}$$

The normalized pressure equation is obtained, function of the j Agents of Change $\phi^+_{\dot{P},j}$ which define the processes acting on $\dot{P}$:

$$\left.\frac{dP^+}{dt}\right|_{prz} = - \omega_{\dot{P},Q_{l,prz,out}} \cdot \phi^+_{\dot{P},Q_{l,prz,out}} - \omega_{\dot{P},Q_{v,prz,out}} \cdot \phi^+_{\dot{P},Q_{v,prz,out}} + \omega_{\dot{P},Q_{prz,heaters}} \cdot \phi^+_{\dot{P},Q_{prz,heaters}} + \omega_{\dot{P},Q_{prz,ow}} \cdot \phi^+_{\dot{P},Q_{prz,ow}} \tag{19}$$

$$\begin{aligned}\left.\frac{dP^+}{dt}\right|_1 = {} & \omega_{\dot{P},Q_{l,HPIS}} \cdot \phi^+_{\dot{P},Q_{l,HPIS}} + \omega_{\dot{P},Q_{cond,HPIS}} \cdot \phi^+_{\dot{P},Q_{cond,HPIS}} - \omega_{\dot{P},Q_{l,break}} \cdot \phi^+_{\dot{P},Q_{l,break}} - \omega_{\dot{P},Q_{v,break}} \cdot \phi^+_{\dot{P},Q_{v,break}} \\ & + \omega_{\dot{P},Q_{core}} \cdot \phi^+_{\dot{P},Q_{core}} + \omega_{\dot{P},Q_{1,ow}} \cdot \phi^+_{\dot{P},Q_{1,ow}} - \omega_{\dot{P},Q_{SG}} \cdot \phi^+_{\dot{P},Q_{SG}}\end{aligned} \tag{20}$$

From equations (8), (9), (19) and (20), the time scaling for relative importance of agents [5] is carried out. The FRC are divided by the dominant one. The effect metrics are obtained thanks to this process, denoting the rate of change due to the contribution of Agents of Change:

$$\Omega_{\dot{M},\chi_j} = \frac{\omega_{\dot{M},\chi_j}}{\left|\omega_{\dot{M},\chi_D}\right|} \quad ; \quad \Omega_{\dot{P},\chi_j} = \frac{\omega_{\dot{P},\chi_j}}{\left|\omega_{\dot{P},\chi_D}\right|} \tag{21}$$

3.3. Results of the a posteriori scaling analysis using the code simulation

Figure 3 displays the primary and secondary pressure evolution from experimental data and CATHARE simulation. The CATHARE code predicts the pressure evolution rather well. Figure 4 details the pressure evolution during the blowdown phase and during the primary-secondary pressure reversal. In Figure 5 the break mass flow rate is rather well predicted with a delay of the transition to HQMD and a higher flow at the end of accumulator discharge, which are not yet discussed in this work.

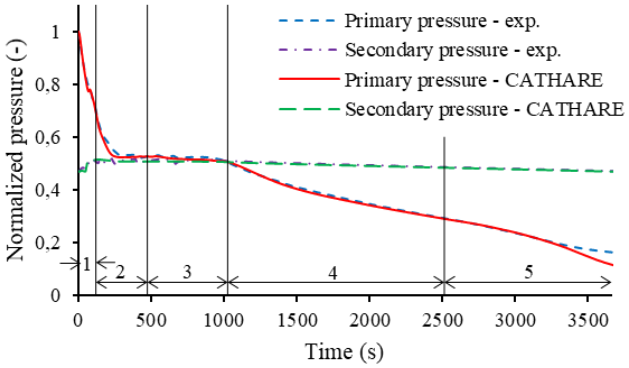

Figure 3. Primary and secondary pressures evolution for the LSTF ROSA 1.2 test

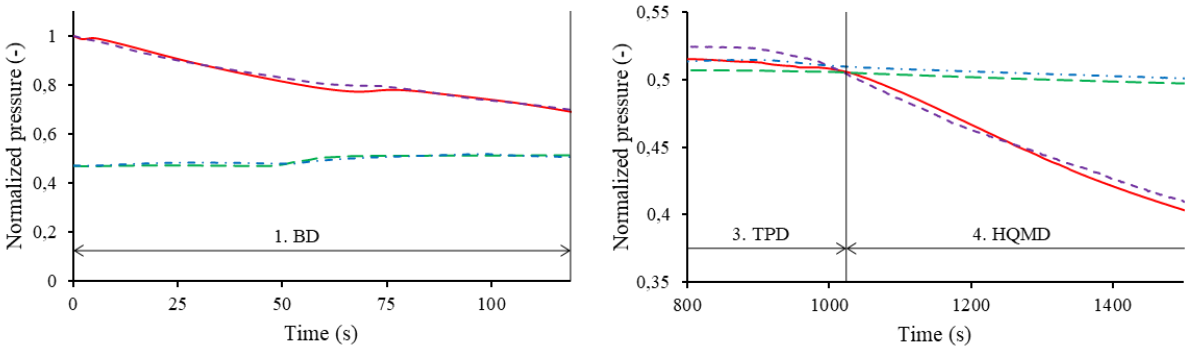

Figure 4. Primary and secondary pressures during BD and during pressure reversal

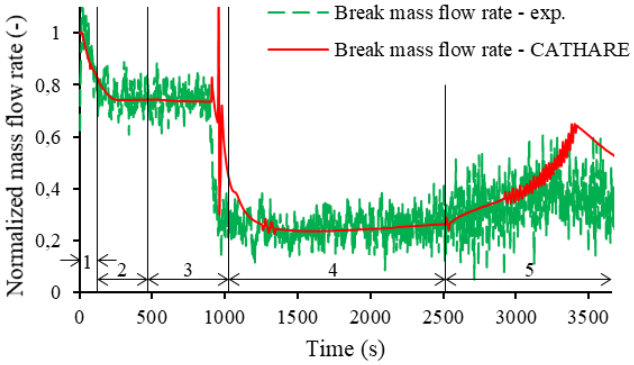

Figure 5. Break mass flow rate evolution for the LSTF ROSA 1.2 test

The good predictions of pressure and break flow rate demonstrate the quality of the CATHARE code (less than 1% error for pressures and less than 4% for flow rate in BD and HQMD phases). It can then be used as a support to the scaling analysis. Main parameters of the study are shown in Table II.

Table II. Main parameters of the BD and HQMD phases of the LSTF ROSA 1.2 test

	1. BD	4. HQMD	
Initial primary mass $M_{1,0}$	5642	2044	kg
Initial pressurizer mass $M_{prz,0}$	508	-	kg
Phase duration Δt	119	1484	s
Primary mass variation ΔM_1	652	58.6	kg
Pressurizer mass variation ΔM_{prz}	434	-	kg
Pressure variation during the phases ΔP	$4.80 \cdot 10^6$	$3.34 \cdot 10^6$	Pa
Averaged mass flow rate at the break $\bar{\dot{M}}_{break}$	5.38	1.56	kg/s
Averaged mass flow rate leaving the pressurizer $\bar{\dot{M}}_{prz}$	3.59	-	kg/s
Averaged mass flow rate of the HPIS $\bar{\dot{M}}_{HPIS}$	-	1.52	kg/s
Averaged core power $\bar{W}_{core}$	$8.34 \cdot 10^6$	$1.37 \cdot 10^6$	W
Averaged pressurizer heaters power $\bar{W}_{prz,heaters}$	$8.50 \cdot 10^4$	-	W
Averaged SG tubes heat exchanges $\bar{W}_{SG}$	$-8.30 \cdot 10^6$	$1.05 \cdot 10^4$	W
Averaged primary wall heat exchanges $\bar{W}_{1,ow}$	$3.86 \cdot 10^4$	$1.84 \cdot 10^5$	W
Averaged pressurizer wall heat exchanges $\bar{W}_{prz,ow}$	$1.42 \cdot 10^5$	-	W

The values of the effect metrics for the mass equation $\Omega_{\dot{M},j}$ and the pressure equation $\Omega_{\dot{P},j}$ are displayed respectively for the blowdown and high-quality mixture discharge phases in Table III and Table IV.

Table III. Effect Metrics for the LSTF ROSA 1.2 test during the BD phase

Rate of mass change in V_{prz} due to the contribution by:		
Liquid flow rate leaving the pressurizer	$\Omega_{\dot{M}_{l,prz,out}}$	1.000
Vapour flow rate leaving the pressurizer	$\Omega_{\dot{M}_{v,prz,out}}$	0.039
Rate of pressure change in V_{prz} the due to the contribution by:		
Liquid flow rate leaving the pressurizer	$\Omega_{\dot{P},Q_{l,prz,out}}$	1.000
Vapour flow rate leaving the pressurizer	$\Omega_{\dot{P},Q_{v,prz,out}}$	0.329
Thermal expansion by vaporization due to the pressurizer heaters	$\Omega_{\dot{P},Q_{prz,heaters}}$	0.159
Thermal expansion by condensation/vaporization due to wall heat exchanges in the pressurizer	$\Omega_{\dot{P},Q_{prz,ow}}$	0.265
Rate of mass change in V_1 due to the contribution by:		
Liquid flow rate leaving the primary system through the break	$\Omega_{\dot{M}_{l,break}}$	1.000
Vapour flow rate leaving the primary system through the break	$\Omega_{\dot{M}_{v,break}}$	0.002
Rate of pressure change in V_1 due to the contribution by:		
Liquid flow rate leaving the primary system through the break	$\Omega_{\dot{P},Q_{l,break}}$	0.100

Vapour flow rate leaving the primary system through the break	$\Omega_{\dot{P},Q_{v,break}}$	0.002
Thermal expansion by vaporization due to the core heat generation	$\Omega_{\dot{P},Q_{core}}$	1.000
Thermal expansion by condensation/vaporization due to SG tubes heat exchanges	$\Omega_{\dot{P},Q_{SG}}$	0.995
Thermal expansion by condensation/vaporization due to wall heat exchanges in the primary system	$\Omega_{\dot{P},Q_{1,ow}}$	0.005

For the pressurizer control volume, the effect metrics that govern the mass and pressure change are those related to the flow rate leaving the pressurizer, which is close to the flow rate to the break. This was also observed by the UPV with the H2TS method. The scaling of the break flow rate should then respect the volume scale ratio. Since the choke flow mass flux is almost independent on the break diameter, this means that a good break scaling should apply the volume scaling factor to the break area. The effect metrics related to the pressurizer heaters and wall heat exchanges can be considered as influents. The UPV has instead taken into account a net heat term obtained from the subtraction of the pressurizer heat losses to the heat provided by the heaters [8]. Their corresponding scaling criteria (from π-monomial) has a value of 0.160. An effect metric of 0.158 is obtained with the same net heat calculation and with their assumptions. As shown by the UPV when comparing LSTF data to reactor scale calculation, the distortion of this contribution of the external pressurizer wall is large. It could be then considered that a pressurizer scaling which would not respect the height (e.g. by adopting a linear scaling) would be better for this LOCA blowdown phase. Note that the design of the LSTF pressurizer has been revised to simulate that of the AP1000 and is relatively larger than that of the conventional Westinghouse PWR. It can also be noted that in the CATHARE code calculation, the vapour mass flow rate leaving the pressurizer is negligible but its volume flow rate is a significant contribution to pressure decrease. It may then be considered that a 0-D modelling of the pressurizer is not sufficiently precise to predict the entrainment of bubbles from pressurizer to the surge line (SL) and to the hot leg. This vapour is due to flashing of the water and it may be expected a gradient of void fraction from bottom to the level with a minimum value at the connection to the SL. A too simple 0-D modelling of the pressurizer may overestimate this void fraction and the vapour flow rate entrained in SL. This is an example showing how an a posteriori scaling analysis with a system code may help improving the modelling when necessary.

Regarding the primary system control volume, the dominant effect metric on the rate of mass change is the one related to the liquid flow rate at the break with a very small contribution of the vapour break flow. Although this repartition cannot be confirmed by measured data, this evaluation is easily accepted since almost only liquid water flows in the loops and pressure vessel. It can be observed on the rate of pressure change that the two processes related to heat exchange in the core and the SG tubes are dominant and almost compensate each other. The liquid volume flow rate at the break can be considered as influent. The vapour volume flow rate and wall heat exchanges are negligible during the blowdown.

Table IV. Effect Metrics for the LSTF ROSA 1.2 test during the HQMD phase

Rate of mass change in V_1 due to the contribution by:		
Liquid flow rate entering the primary system thanks to HPIS	$\Omega_{\dot{M}_{l,HPIS}}$	1.000
Liquid flow rate leaving the primary system through the break	$\Omega_{\dot{M}_{l,break}}$	0.802
Vapour flow rate leaving the primary system through the break	$\Omega_{\dot{M}_{v,break}}$	0.225
Rate of pressure change in V_1 due to the contribution by:		
Liquid flow rate entering the primary system thanks to HPIS system	$\Omega_{\dot{P},Q_{l,HPIS}}$	0.062
Thermal expansion by condensation due to the liquid flow rate entering the primary system thanks to HPIS system	$\Omega_{\dot{P},Q_{cond,HPIS}}$	1.000

Liquid flow rate leaving the primary system through the break	$\Omega_{\dot{P},Q_{l,break}}$	0.050
Vapour flow rate leaving the primary system through the break	$\Omega_{\dot{P},Q_{v,break}}$	0.356
Thermal expansion by vaporization due to the core heat generation	$\Omega_{\dot{P},Q_{core}}$	0.862
Thermal expansion by condensation/vaporization due to SG tubes heat exchanges	$\Omega_{\dot{P},Q_{SG}}$	0.007
Thermal expansion by condensation/vaporization due to wall heat exchanges in the primary system	$\Omega_{\dot{P},Q_{l,ow}}$	0.116

During the high-quality mixture discharge phase, the total contribution of the break mass flow rates to the primary mass is almost compensated by the HPIS.

The three most important effect metrics for the rate of pressure change are the one related to the HPIS, to the core heat generation and to the break (mainly the vapour flow rate). The UPV gives a contribution from HPIS of 0.498. Having assumed here a saturation state overestimate the condensation of HPIS water. Further analysis will be done using Eq. (12) to better estimate the condensation. The UPV analysis found the net heat term (heat balance between the core, the SG tubes and the losses [8]) as the dominant term. It is actually observed that the SG tubes exchanges term is negligible. Contributions of the wall heat exchanges can be considered as influent. On the contrary, their value relative to the vapour flow rate is almost zero while the analysis here gives a value of 0.356. These differences could be explained by the nature of the corresponding terms in the pressure equations, which do not refer exactly to the same quantities.

An order of magnitude analysis of the terms of the pressure equation assuming saturation conditions (15) can estimates the expansion coefficient K_s at the moment of the primary-secondary pressure reversal. It is found that the equation is not exactly balanced probably because the saturation assumption is not respected.

The comparative analysis of these methods carried out here shows that they are based on the same methodological approaches:

- The same normalization concept of the contributing terms of the balance equations are used. The H2TS and FSA methods suggest the use of boundary conditions for this normalization.

- A normalization via averaged quantities using the CATHARE calculation is made. This is more representative of the evolution of the contributing values over the phases, for example, by averaging the heat exchanges and flow rates terms.

- The two methods calculate scaling criteria but in different ways. The π-monomial in the H2TS and the effect metrics in the FSA. To calculate them, scaling methods take into account the ratio of the indicators of the intensities of the processes over the studied variable.

- To identify the scaling criteria and therefore distortions, H2TS performs time scaling through a characteristic time for the variable evolution. This characteristic time is the ratio between the control volume and the convective volumetric flow rate [4][8]. The equivalence in FSA corresponds to the time scaling for relative importance of agents. Since FRC takes into account the characteristic time of the processes, dimensionless effect metrics are directly linked to the dominant process [5]. As mentioned in [1] where a comparison of H2TS and FSA is also carried out: “The FSA determines scale distortion quantitatively from the ratios of fractional rate changes for each specific agent of change. H2TS computes scale distortion by taking ratios of dimensionless characteristic-time ratios.” This addition to this newer method is perhaps a way to better scale the time.

4. CONCLUSIONS

An a posteriori scaling analysis is here applied to the ROSA 1.2 hot leg SB-LOCA test performed on the Japanese LSTF-ROSA-IV facility. The FSA method is applied here to selected equations. And for those equations, we evaluate the term values with the CATHARE code simulations. Attention is first focused on the blowdown and high-quality mixture discharge phases of this SB-LOCA. Mass and pressure equations on the pressurizer and primary system volumes are defined and applied to the methodology. This work intends to provide a comparison between the results of the FSA with the one obtained by the UPV with the H2TS and to see how these methods can be applied with the support of the system codes which have now a good maturity and a reasonable level of confidence.

The formulation of pressure equation for the pressurizer and for the primary circuit as a volume rate of change equation helps giving a clear physical meaning to each contributor. Any fluid volume source (resp. sink) contributes to pressurization (resp. depressurization). Any heating (resp. cooling) contributes to pressurization (resp. depressurization). Since the volume is constant, any imbalance between heating, cooling, fluid volume sources and sinks is compensated by a fluid volume expansion or contraction by pressure decrease or increase.

Several common aspects may be found in H2TS and FSA. The FSA may be seen as an improvement of the older H2TS method [1]. As shown by the application made here, the results obtained by the two methods are similar when the nature of the equations is equivalent. The most important is not the method itself but the choice of equations, the possible simplifications that are used, and the way to evaluate each term. Their choice is therefore essential for the qualitative study of a transient. In addition, the FSA improvements are likely to provide better temporal analysis. Moreover, it is here believed that the use of mature scaling code to better evaluate terms of the equation may be of interest.

From the first results of this scaling analysis, the hierarchy of the processes acting on mass and pressure change during the blowdown and the high-quality mixture discharge phases is established. All methods identify the same scaling criteria to apply to power and to break area. All methods identify distortions due to heat exchanges with solids (other than fuel rods and SG tubes). Surprisingly no ITF which used the power to volume scaling and full height scaling (i.e. BETHSY, LSTF, LOBI, SPES), adopted another scaling criterion for the pressurizer which would minimize the distortion by using a reduced height of this component only.

The use of a mature and extensively validated system code – here the CATHARE code – allows the user of the method to limit the assumptions about the values chosen for the study. The code actually provides additional precision by averaging these values rather than relying in estimations at boundary of the phases. System codes can now support scaling analyses. It may be of interest to apply the scaling first with the original FSA method and then to revisit it by re-evaluating the terms using a system code simulation.

Moreover, scaling methods can also support the improvement of the code modelling as shown in the pressurizer pressure equation analysis for the blowdown phase.

This work will continue by analyzing the five phases and by using the pressure equation formulated without saturation assumption. It will be more precise but some instruments must be implemented in the system code to store the value of each term.

NOMENCLATURE

Acronyms

AIS	Accumulator Injection System
BD	Blowdown Discharge
CATHARE	“Code Avancé de THermohydraulique pour les Accidents de Réacteurs à Eau”
CL	Cold Leg
FoM	Figure of Merit
FRC	Fractional Rate of Change
FSA	Fractional Scaling Analysis
H2TS	Hierarchical Two Tiered Scaling
HQMD	High Quality Mixture Discharge
HL	Hot Leg
HPIS	High Pressure Injection System
IET	Integral Effect Test
ITF	Integral Test Facility
JAERI	Japan Atomic Energy Research Institute
SB-LOCA	Small Break Loss Of Coolant Accident
LSC	Loop Seal Clearing
LSP	Loop Seal Plugging
LSTF	Large Scale Test Facility
NC	Natural Circulation
PCT	Peak Clad Temperature
PIRT	Phenomena Identification and Ranking Table
PoI	Parameter of Interest
PRZ	Pressurizer
PWR	Pressurized Water Reactor
RCM	Reflux Condenser Mode
RR	Reactor Refilling
ROSA	Rig Of Safety Assessment program
RPV	Reactor Pressure Vessel
SCRAM	Safety Control Rod Axe Man
SG	Steam Generator
SL	Surge Line
TMI	Three Miles Island accident
TRACE	TRAC/RELAP Advanced Computational Engine
TPD	Two-Phase Discharge
UPV	Universidad Politecnica de Valencia
VRC	Volume Rate of Change

Symbols

A	Area	m^2
e	Specific internal energy	J/kg
h_k	Local specific enthalpy of phase k	J/kg
$h_{ks,p}'$	Derivative of specific enthalpy of phase k at saturation with respect to pressure	m^3/kg
$h_{l,in}$	Specific enthalpy of the liquid mass flow rate entering the control volume	J/kg
$h_{v,in}$	Specific enthalpy of the vapour mass flow rate entering the control volume	J/kg
H_k	Volume averaged specific enthalpy of phase k	J/kg
K_s	Global expansion coefficient	m^3/Pa
M_k	Mass of the phase k in the control volume	kg
$\dot{M}_k$	Rate of change of the mass of phase k in the control volume	kg/s
$\dot{M}_{l,in}$	Liquid mass flow rate entering the control volume	kg/s
$\dot{M}_{v,in}$	Vapour mass flow rate entering the control volume	kg/s
$\dot{M}_{l,out}$	Liquid mass flow rate flowing out of the control volume	kg/s
$\dot{M}_{v,out}$	Vapour mass flow rate flowing out of the control volume	kg/s
p	Local pressure	Pa
P	Pressure of the control volume	Pa
$\dot{P}$	Rate of change of the pressure in the control volume	Pa/s
q	Power sources	W
Q	Volume rate of change	m^3/s
t	Time	s
V	Control Volume	m^3
Y	Thermophysical property	-
$W_{w,l}$	Wall-to-liquid heating or cooling power exchanged	W
$W_{w,v}$	Wall-to-vapour heating or cooling power exchanged	W
W_{wi}	Wall-to-interface heating or cooling power related to boiling or condensation	W
$W_{i,l}$	Interface-to-liquid heating or cooling power exchanged	W
$W_{i,v}$	Interface-to-vapour heating or cooling power exchanged	W
v_k	Specific volume of phase k	m^3/kg
v_{ks}	Specific volume of phase k at saturation	m^3/kg
$v'_{k,p}$	Partial derivative of specific volume of phase k with respect to pressure	$m^4.s^2/kg^2$
$v'_{k,h}$	Partial derivative of specific volume of phase k with respect to enthalpy	$m.s^2$/kg
ρ	Density	kg/m^3
u	Velocity	m/s
ϕ	Agent of Change	-
ω	Fractional Rate of Change	s^{-1}
Ω	Effect metric	-

Subscripts and superscripts

1	Related to primary system	l	Related to liquid phase
prz	Related to pressurizer	v	Related to vapour phase
s	Saturation conditions	i	Related to interface
0	Initial/reference value	w	Related to walls
in	Inlet	ow	Related to other walls than core and SG
out	Outlet	$\cdot$	Variation over time
+	Dimensionless variable	$-$	Averaged value

REFERENCES

1. D. Bestion, F. D'Auria, F. Lien and H. Nakamura, "A state-of-the-art report on scaling in system thermal hydraulics applications to nuclear reactor safety and design" *Nuclear Safety*, NEA/CSNI/R(2016)14 (2017).
2. M. Ishii, S.T. Revankar, T. Leonardi, R. Dowlati, M.L. Bertodano, I. Babelli, W. Wang, H. Pokharna, V.H. Ransom, R. Viskanta and J.T. Han, "The three-level scaling approach with application to the Purdue University Multi-Dimensional Integral Test Assembly (PUMA)" *Nuclear Engineering and Design* **186**, pp. 177-211 (1998).
3. T.-J. Liu, C.-H. Lee and C.-Y. Chang, "Power-operated relief valve stuck-open accident and recovery scenarios in the Institute of Nuclear Energy Research integral system test facility" *Nuclear Ensgineering and Design* **186**, pp 149-176 (1997).
4. N. Zuber, "A hierarchical, Two-tiered Scaling Analysis, Appendix D of An Integrated Structure and Scaling Methodology for Severe Accident Technical Issue Resolution" NUREG/CR-5809 (1991).
5. N. Zuber, U. S. Rohatgi, W. Wulff and I. Catton, "Application of fractional scaling analysis (FSA) to loss of coolant accidents (LOCA)" *Nuclear Engineering and Design* **237** pp. 1593-1607 (2007).
6. J. N. Reyes, "The Dynaminal System Scaling Methodology" NURETH-16 (2015).
7. N. Zuber, G.E Wilson, M. Ishii, W. Wulff, B.E Boyack, A.E Dukler, P. Griffith, J. M. Healzer, R. E. Henry, J. R Lehner, S. Levy, F. J. Moody, M. Pilch, B. R. Sehgal, B. W. Spencer, T. G. Theofanous and J. Valente, "An integrated structure and scaling methodology for severe accident technical issue resolution: Development of methodology" *Nuclear Engineering and Design* **186**, pp. 1-21 (1998).
8. J.L. Muñoz-Cobo, C. Berna and A. Escrivá, "Top-down scaling methodology from the LSTF facility to a three loop PWR plant applied to a SBLOCA event – The ROSA 1.2 test" *Nuclear Engineering and Design* **327** pp. 248-273 (2018).
9. R. Préa, P. Fillion, L. Matteo, G. Mauger and A. Mekkas, "CATHARE-3 V2.1: the new industrial version of the CATHARE code" *Advances in Thermal Hydraulics* pp. 730-742 (2020).
10. P. Emonot, A. Souyri, J. L. Gandrille, F. Barré, "CATHARE-3: A new system code for thermal-hydraulics in the context of the NEPTUNE project" *Nuclear Engineering and Design* **241**, pp 4476-4481 (2011).
11. D. Bestion, "The physical closure laws in the CATHARE code" *Nuclear Engineering and Design* **124**, pp 229-245 (1990).
12. OECD/NEA, "Final Integration Report of OECD/NEA ROSA Project (2005-2009)," NEA/CSNI/R(2013)1.
13. The ROSA-V Group, "ROSA-V large scale test facility (LSTF) system description for the third and fourth simulated fuel assemblies" JAERI-Tech (2003).
14. D. Bestion, "About phenomena identification in a PIRT" NURETH-18 (2019).